Simulation of Two-Phase Rayleigh-Benard Problem Using Lattice Boltzmann Method

Armin Haghshenas[1], Mohammad Hassan Rahimian[2]

Department of Mechanical Engineering, College of Engineering, University of Tehran, Tehran, Iran[1,2]

Abstract: In the present work, two-phase Rayleigh-Benard problem is simulated by lattice Boltzmann method. Two horizontal layers of immiscible fluid are confined in a rectangular cavity. The vertical walls of the cavity are insulated while the horizontal walls are maintained at different constant temperatures. Two-phase lattice Boltzmann method is used to model hydrodynamic field and a passive scalar approach is implemented to model the thermal field. The viscous heat dissipation and compression work done by pressure are neglected. The present model is validated with the single-phase Rayleigh-Benard problem and good agreement is observed. The applicability of this new lattice Boltzmann model for simulating thermal two-phase problems is the main objective of this study. Furthermore, a comprehensive parametric study of the problem is carried out for wide range of different non-dimensional parameters. It is found that with increase of Rayleigh number, the fluid motion becomes stronger and the isotherms are more distorted. Also with decrease of the ratio of Prandtl number of upper fluid to lower fluid, conduction dominates in the upper layer. It is concluded that this new thermal lattice Boltzmann model has a great capability to model thermal two-phase problems.

Keywords: Thermal lattice Boltzmann method, Two-phase Rayleigh-Benard problem, Passive scalar approach, Rectangular cavity.

I. INTRODUCTION

Two-phase Rayleigh-Benard (RB) problem occurs when two layers of immiscible fluids which are confined between two horizontal parallel plates, are heated from below and cooled from above. Due to its practical importance in many general science and engineering applications, the problem of two-phase RB has been the subject of many theoretical, experimental, and numerical studies. One can mention, for example, its application in freezing or melting, where the onset of thermal convection and its stability are coupled with the deformable interface. Such is the case for the storage of energy using the melting of material.

As compared to the widely studied one-phase problems [1, 2], not many studies have been reported for two-phase RB problems. Lan et al. [3] investigated the stability and bifurcation of a partially melted or solidified material in a two-phase Rayleigh–Benard problem by a finite-volume/Newton's method. Results were presented for a variety of parameters of interest, including the Rayleigh number, aspect ratio, tilt angle, and also the Prandtl number. Binghong et al. [4] numerically studied Rayleigh-Marangoni-Benard instability in a system of two-layer fluids. They analysed the convective instabilities in the system of Silicon Oil and Fluorinert liquids. The Rayleigh–Marangoni–Benard convective instability in the two-layer systems such as Silicone oil/Fluorinert and Silicone oil/water liquids were studied by Liu et al. [5].

They performed both linear and nonlinear instability analysis to investigate the influence of thermo capillary force on the convective instability of the two-layer system. Also, some numerical studies [6,7] have been applied to two-fluid Rayleigh–Benard problem, but the shape of the interface was assumed to be rigid, flat and horizontal.

Over the last decade, many researchers have made endeavours to enhance the ability of the lattice Boltzmann method (LBM) to simulate multiphase fluid flows. Furthermore, several lattice Boltzmann multiphase flow models have been proposed during this time. Among them are the chromo-dynamic model [8], the pseudo potential model [9, 10], the free-energy-based approach [11], and a consistent multiphase LBM based on the kinetic theory for dense fluids [12]. He and Doolen [13] have reviewed these methods and argued about the weak points and shortcomings of them. Recently, He et al. [14] modified the last mentioned two-phase LBM [12] and applied it in simulation of two-dimensional Rayleigh–Taylor instability without surface tension. Fakhari and Rahimian [15] utilized the mentioned LBE proposed by The et al. to simulate deformation and breakup of a falling drop under gravity. Despite the progress made in simulating multiphase and multi component flows, there is a crucial missing part which is the lack of a satisfactory thermal model for multiphase flows. Most of the published LBM multiphase studies have been restricted to isothermal systems. The most obvious difficulty for thermal LBM is tracking the energy evolution while conserving total energy. In general, the available thermal LB models fall into three categories: the multi-speed approach, passive scalar approach, and hybrid thermal dynamic approach. In the passive-scalar approach, the temperature field is passively advected by the fluid flow and can be simulated as an additional component of the fluid system. This means in order to solve for the temperature field in the multiphase isothermal LBE framework, one only need to solve an auxiliary LBE [16]. This method results in a consistent and integrated solution of the mass, momentum and energy evolution of the system at the continuum level.

However, it has demonstrated that such system suffers severe numerical instabilities and has a limited dynamic range in temperature. In the passive scalar approach, the temperature is treated as a passive scalar, which is carried by the flow field but does not affect it [17,18]. This approach solves the mass and momentum equations with a single distribution function and the energy balance with another. In hybrid thermal dynamic approach, the flow simulation is decoupled from the solution of temperature. Specifically, the flow simulation is accomplished by using a thermal LB equation, while the temperature equation is solved using a traditional CFD method, such as finite-different schemes or other means [19, 20].

Yuan and Schaefer [21, 22] proposed a new and generalized lattice Boltzmann model for simulating thermal two-phase flow. First they described the multiphase isothermal lattice Boltzmann equation model proposed by Shan and Chen and the single phase thermal LBE model (the passive-scalar approach). Then, by combining these two models, the thermal two-phase LBE model was proposed. Chang and Alexander [23] investigated two-fluid Rayleigh-Benard and Marangoni convection by using the hybrid lattice Boltzmann finite-difference simulation. They extended LBM to include the effects of interfacial tension and its dependence on temperature and applied it to the mentioned problem. A parametric study of the effects of thermally induced density change, buoyancy, surface tension variation with temperature on interface dynamics, flow regimes and heat transfer were presented.

In the present study, a two-phase LBM proposed by He et al. [14] is combined with a passive scalar approach to simulate non-isothermal two-phase Rayleigh-Benard problem. To the best of our knowledge, the applicability of such a combination has not been investigated; therefore, the main objective of this study is to see whether this Thermal lattice Boltzmann model (TLBM) can be used efficiently to model non-isothermal two-phase problems. We are particularly interested in studying the effects of parameters such as Rayleigh number, Prandtl number and parameter ε which is the multiple of thermal expansion coefficient and temperature difference. The outline of the work is as follows: First, a brief description is given of the governing equations, the numerical strategy, and boundary conditions. Next, the code validation will be performed and then, results are reported and discussed. Finally, some conclusions are drawn.

II. PHYSICAL PROBLEM AND MATHEMATICAL FORMULATION

The present numerical investigation considers two horizontal layers of immiscible fluid, confined in a rectangular cavity with aspect ratio of 2 (L/H=2), the thickness of the lower fluid layer is h_h; the upper layer h_l, and the thickness ratio of layers is equal by one. The vertical walls are insulated while the horizontal walls are maintained at different constant temperatures.

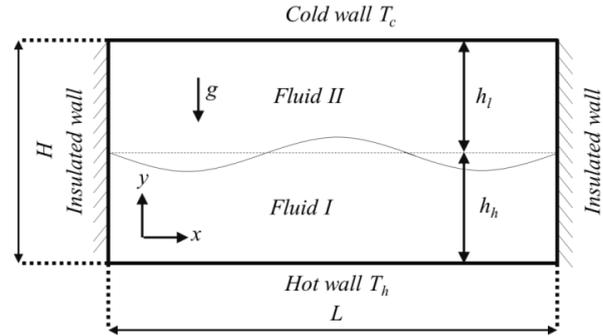The configuration and the boundary conditions are illustrated in Fig.1.

Fig. 1 Schematic illustration of the problem under consideration

Some assumptions have been made in this work, such as:
- Two layers of fluids are perfectly immiscible.
- The interface is deformable.
- Convection is in two dimensions.
- Fluids are incompressible with Boussinesq approximation.
- The viscous heat dissipation and compression work done by pressure are neglected.

An easy way to comply with the conference paper formatting requirements is to use this document as a template and simply type your text into it.

A. Isothermal Multiphase LBE Model

The mathematical demonstration of the isothermal multiphase LBE can be found in Fakhari and Rahimian [15]. Starting from the Boltzmann equation with a proper incompressibility approximation, the f evolution equations for the index distribution function, which is used to track the interface, and the pressure distribution function g, by which the hydrodynamic properties are calculated, obtain as:

$$\bar{f}_\alpha(\mathbf{x}+\mathbf{e}\delta_t, t+\delta_t) = \bar{f}_\alpha(\mathbf{x},t) - \frac{\bar{f}_\alpha - f_\alpha^{eq}}{\tau} - \frac{2\tau-1}{2\tau}\frac{(\mathbf{e}_\alpha - \mathbf{u})\nabla\psi(\varphi)}{RT_0}\Gamma_\alpha\delta_t$$

$$\bar{g}_\alpha(\mathbf{x}+\mathbf{e}\delta_t, t+\delta_t) = \bar{g}_\alpha(\mathbf{x},t) - \frac{\bar{g}_\alpha - g_\alpha^{eq}}{\tau} + \frac{2\tau-1}{2\tau}(\mathbf{e}_\alpha - \mathbf{u})\times \qquad 1$$
$$[\Gamma_\alpha(\mathbf{F}_s + \mathbf{G}) - (\Gamma_\alpha - w_\alpha)\nabla\psi(\rho)]\delta_t$$

where $\mathbf{x}$ is the position vector, t stands for time, R is the gas constant, T is the temperature, T_0 is the average temperature, $\mathbf{e}_\alpha$ denotes the discrete velocity set, $\mathbf{u}$ is the macroscopic velocity, τ is the relaxation time, and $\mathbf{F}_s$ is the surface tension force which is calculated using:

$$\mathbf{F}_s = \kappa\rho\nabla\nabla^2\rho \qquad 2$$

Function Γ_α takes the following form:

$$\Gamma_\alpha = w_\alpha\left[1 + 3\frac{(\mathbf{e}_\alpha\mathbf{u})}{c^2} + 4.5\frac{(\mathbf{e}_\alpha\mathbf{u})^2}{c^4} - 1.5\frac{\mathbf{u}^2}{c^2}\right] \qquad 3$$

We chose δx = δt = 1 hence c=δx/δt=1 and c_s^2=RT_0=1/3. The microscopic velocities and weight coefficients defined as:

$$e_\alpha = \begin{cases} 0 & \alpha = 0 \\ (\cos\theta, \sin\theta) & \theta = (\alpha-1)\pi/2, & \alpha = 1,2,3,4 \\ \sqrt{2}(\cos\theta, \sin\theta) & \theta = (\alpha-5)\pi/2 + \pi/4, & \alpha = 5,6,7,8 \end{cases} \qquad 4$$

$$w_\alpha = \begin{cases} \dfrac{4}{9}, & \alpha = 0 \\[2mm] \dfrac{1}{9}, & \alpha = 1,2,3,4 \\[2mm] \dfrac{1}{36}, & \alpha = 5,6,7,8 \end{cases} \qquad 5$$

The equilibrium distribution functions are related to Γ_α through

$$f_\alpha^{eq} = \varphi \Gamma_\alpha$$
$$g_\alpha^{eq} = \rho RT\, \Gamma_\alpha + (p - \rho RT)w_\alpha \qquad 6$$

The function $\psi(\varphi)$ in Eq. (1) represents the non-ideal part of equation of state (EOS). Using the Carnahan–Starling equation of state, $\psi(\varphi)$ can be expressed as:

$$\psi(\varphi) = \varphi^2 RT \frac{4 - 2\varphi}{(1-\varphi)^3} - a\varphi^2 \qquad 7$$

Where the parameter a determines the strength of the molecular interaction. In order to ensure phase segregation, a must be chosen such that $a > 10.601RT_0$. In this study $a = 12RT_0$ is used. Note that $\psi(\rho)$ in Eq. (1) must be calculated from the macroscopic pressure by

$$\psi(\rho) = p - \rho RT_0 \qquad 8$$

In 2D, the macroscopic variables are calculated using the following relations:

$$\varphi = \sum_{\alpha=0}^{8} \bar{f}_\alpha$$
$$p = \sum_{\alpha=0}^{8} \bar{g}_\alpha - \frac{\mathbf{u}.\nabla \psi(\rho)}{2}\delta_t \qquad 9$$
$$\rho RT\mathbf{u} = \sum_{\alpha=1}^{8} \bar{g}_\alpha \mathbf{e}_\alpha + \frac{RT_0}{2}(\mathbf{F}_s + \mathbf{G})\delta_t$$

The density of the fluid may be obtained by a simple interpolation:

$$\rho(\varphi) = \rho_l + \frac{\varphi - \varphi_l}{\varphi_h - \varphi_l}(\rho_h - \rho_l) \qquad 10$$

Where ρ_l and ρ_h are densities of light and heavy fluids, respectively, and φ_l and φ_h are the minimum and maximum values of the index function, respectively. In the present study $\varphi_l = 0.022838$ and $\varphi_h = 0.250291$ are used as the limiting values of index function. The kinematic viscosity is related to the dimensionless relaxation time by:

$$\nu = (\tau - 0.5)RT_0\delta_t \qquad 11$$

B. Multiphase Thermal LBE Model
In order to take thermal effects into account, we utilize the passive-scalar approach. If the viscous and compressive heating effects are negligible, the temperature field satisfies a much simpler passive-scalar equation:

$$\frac{\partial T}{\partial t} + \mathbf{u}.\nabla T = \nabla.(\alpha \nabla T) + \chi \qquad 12$$

Where $\mathbf{u}$ is the whole fluid velocity, α is the thermal diffusivity, and χ is the source term.
Eq. (12) can be solved in the LB framework by using an additional distribution function.

$$\bar{h}_\alpha(\mathbf{x} + \mathbf{e}\delta_t, t + \delta_t) = \bar{h}_\alpha(\mathbf{x},t) - \frac{1}{\tau_t}\left[\bar{h}_\alpha(\mathbf{x},t) - h_\alpha^{eq}(\mathbf{x},t)\right] \qquad 13$$

$$h_\alpha^{eq} = Tw_\alpha\left(1 + 3(\mathbf{e}_\alpha.\mathbf{u}) + \frac{9}{2}(\mathbf{e}_\alpha.\mathbf{u})^2 - \frac{3}{2}\mathbf{u}^2\right) \qquad 14$$

$$T = \sum_{\alpha=0}^{8} \bar{h}_\alpha \qquad 15$$

It has to be noted that τ_t (the dimensionless single relaxation time for temperature) is calculated using the following equation:

$$\Pr = \frac{\nu}{\alpha} = \frac{2\tau - 1}{2\tau_t - 1} \qquad 16$$

The important non-dimensional parameters of this problem for heavy fluid are such as:

Rayleigh number: $Ra_h = \dfrac{g\beta_h \Delta T H^3 \Pr_h}{\nu_h^2}$

Capillary number: $Ca_h = \dfrac{\rho_h \nu_h \sqrt{g\beta_h \Delta T H}}{\sigma}$

Prandtl number: $\Pr_h = \dfrac{\nu_h}{\alpha_h}$

$\varepsilon_h = \beta_h \Delta T$

Where H is the width of the rectangular cavity and $\Delta T = T_h - T_c$, in which T_h and T_c are the bottom and top wall temperatures, respectively ($T_h > T_c$).
The average Nusselt number along the horizontal line of $y = y_0$ is defined by:

$$Nu_{avg}\Big|_{y=y_0} = -\frac{H}{L\Delta T}\int \frac{\partial T}{\partial y}\Big|_{y=y_0} dx \qquad 17$$

In this model, the fluid dynamics are simulated by an isothermal two-phase LBM proposed by He et al. and the temperature field is determined by an additional passive-scalar equation. The coupling of these two parts is through a suitably defined body force term in the isothermal LBE model.
In dealing with this body force, the Boussinesq approximation is adopted, which assumes that the material properties are independent of temperature except in the body force term where the fluid density is assumed $\rho = \rho_i$ [1- $\beta_i(T-T_{ref})$]. The effective additional thermal buoyancy force after absorbing the term of $\rho_i \mathbf{g}$ into the pressure can be written as:

$$\mathbf{G}_1 = -\rho_i \beta_i (T - T_{ref})\mathbf{g} \qquad 18$$

Where $T_{ref} = (T_h + T_c)/2$, ρ_i is either ρ_h for the heavy fluid at T_{ref} or ρ_l for the light fluid at T_{ref}, β_i is the coefficient of thermal expansion of fluid i, and $\mathbf{g}$ is gravitational acceleration. An additional body force term arises due to the phase buoyancy force related to the density jump across a phase boundary caused by different phases can be given as:

$$\mathbf{G}_2 = (\rho - \rho_{ref})\mathbf{g} \qquad 19$$

Where ρ_{ref} is the average density of the two-fluid system at T_{ref}, ($\rho_{ref} = (\rho_h + \rho_l)/2$). Therefore, the total body force term is the sum of phase and thermal buoyancy forces.
The last thing remained to be done is the implementation of the boundary conditions which is indeed very important

for our LBM simulation. To that end, at each time step, the distribution functions pointing to the inner zone at the boundary nodes must be specified. Regarding the no-slip boundary condition, bounce-back boundary condition is applied on walls for distribution functions of f and g, i.e.:

$$\bar{f}_\alpha(\mathbf{x},t) = \bar{f}_\beta(\mathbf{x},t)$$
$$\bar{g}_\alpha(\mathbf{x},t) = \bar{g}_\beta(\mathbf{x},t)$$

20

Here α and β indicate opposite directions.

To determine the unknown temperature distribution functions at each step, boundary condition proposed by Inamuro et al. [25] is used.

1) Horizontal walls: Suppose the temperature is fixed as TB at the bottom wall. After streaming, h2, h5, and h6 are unknowns. Assume these unknown PDFs equal their equilibrium distribution given by Eq. (14) with T replaced by unknown temperature T′. Summing these three PDFs together, we have:

$$\bar{h}_2 + \bar{h}_5 + \bar{h}_6 = \frac{1}{6}T'\left(1 + 3u_y + 3u_y^2\right)$$

21

Where, u_y is the velocity normal to the wall. If we know T′, we will be able to solve for h_2, h_5, and h_6. Meanwhile, we notice that for the isothermal wall, $\sum h = T_B$.

Substituting Eq. (21) into this, T′ can be calculated as follows:

$$T' = \frac{6}{1 + 3u_y + 3u_y^2}\left(T_B - \bar{h}_0 - \bar{h}_1 - \bar{h}_3 - \bar{h}_4 - \bar{h}_7 - \bar{h}_8\right)$$

22

Finally, h_2, h_5, and h_6 can be obtained by substituting T′ into Eq. (14).

2) Vertical walls: A second-order finite difference scheme is used to get the temperature on the wall, after finding the wall temperature, the same procedure as described in the horizontal wall case is used to calculate the unknown PDFs.

III.RESULTS AND DISCUSSIONS

To ensure that the LBM code is working properly, the problem of single-phase Rayleigh-Benard in a rectangular cavity is modelled and compared with the results reported by Clever et al. [26], and Prasianakis et al. [27].

To model single-phase RB problem, we need to choose all the dimensionless ratio of the fluid properties in our two-phase code near to one. Furthermore, the vertical walls are removed and periodic boundary condition is implemented. Table I compares the average Nusselt numbers obtained in the present work with those reported in the literature.

Table I Papers Comparison between Our Numerical Results with Published Data for Single-Phase RB Problem in a Rectangular 2d Cavity

Rayleigh Number	5×10^3	10^4	5×10^4
	Average Nusselt Number at Hot Wall		
Clever et al. [26]	2.116	2.661	4.245
Prasianakis et al. [27]	2.104	2.644	4.133
Present work	2.121	2.655	4.191

As it can be seen in table I, in each case, the results are considerably consistent with those in the literature and these comparisons corroborate the employed numerical method, which can produce reliable results. Also, streamlines and isotherms for single-phase RB problem for Ra=10^4, Pr=0.71 are shown in Fig. 2.

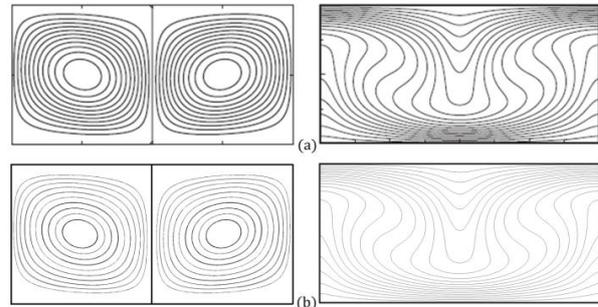Fig. 2 Streamlines and isotherms for single-phase Rayleigh Benard problem for Ra=10^4, Pr=0.71

Having validated the code, we are now at a stage to present our brand new results for two-phase Rayleigh-Benard problem. Each fluid is characterized by its kinematic viscosity v_i, thermal expansion coefficient β_i, thermal diffusivity α_i, and volumetric mass density ρ_i. The dimensionless ratio of the fluid properties are $\rho_r = \rho_l/\rho_h = 0.33$ (density), $v_r = v_l/v_h = 1.0$ (kinematical viscosity), $\beta_r = \beta_l/\beta_h = 2.0$ (coefficient of thermal expansion), $\alpha_r = \alpha_l/\alpha_h = 1.0$ (thermal diffusivity). Initially, thickness of two-layer fluids is equal, $h_l = h_h = 0.5H$. Simulation is carried out on a 401 by 201 grid. Grid independence of the results has been established. The variations of the average Nusselt number at hot and cold walls with changing grid size are shown in Table II.

Table II Grid-Dependence Study For Two-Phase Rayleigh-Benard Problem With Rah=5×104, Prr=1, Eh=0.1

Mesh	201×101	301×151	401×201	501×251
Nu$_{avg}$ at hot wall	2.326	2.360	2.367	2.370
Nu$_{avg}$ at cold wall	2.329	2.360	2.364	2.366

The maximum change in this metrics as a result of using the finer mesh is only 1.5%. Hence the results can be taken to be grid independent. Although the results are trustful by 201 102 grid, we carried out the simulation on 401 201 grid to obtain the exact values. It should be noted that with increase of Ra, finer mesh should be utilized, otherwise the program diverges.

A. Effect of Rayleigh number

First, the effect of the Rayleigh number on streamlines and isotherms is investigated. The Capillary number, Prandtl number ratio and ε_1 are held fixed at 4×10^{-4}, 1.0 and 0.1, respectively. The Rayleigh number is varied from 2×10^4 to 2×10^5. Fig. 3 shows the isotherms and streamlines for Ra$_h$=2×10^4, 5×10^4, 10^5 and 2×10^5. As it can be seen in this figure, each layer is occupied by clockwise and counter Clockwise circulating cells and the circulating in the upper
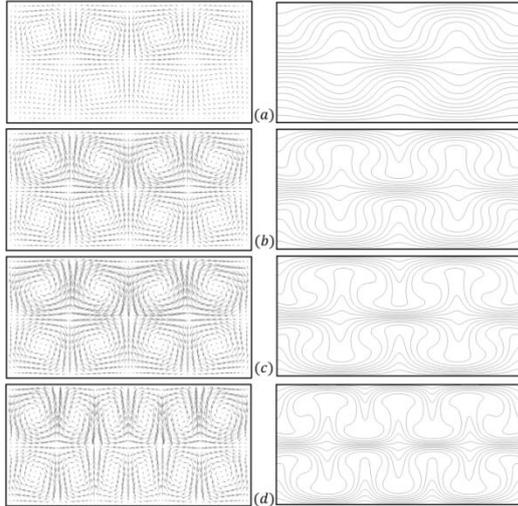
Fig. 3 Streamlines and isotherms for $Ca_h = 4.0 \times 10^{-4}$, $Pr_r = 1.0$, $\varepsilon_h = 0.1$ (a) $Ra_h = 2.0 \times 10^4$, (b) $Ra_h = 5.0 \times 10^4$, (c) $Ra_h = 1.0 \times 10^5$, and (d) $Ra_h = 2.0 \times 10^5$

layer is little stronger than in the lower layer. This phenomenon was expected because the upper fluid has less density and greater thermal expansion coefficient than the lower layer, while their Prandtl numbers and viscosities are the same. As a result of greater thermal expansion coefficient in the upper layer, the buoyancy force is greater in the upper area and also just because its density is less, the temperature changes faster which causes stronger convection and fluid flow.

As Rayleigh number increases, the fluid convection become stronger and the isotherms are more distorted. Furthermore, in each case for $Ra_h < 2 \times 10^5$, there are two pairs of counter-rotating convection rolls both in lower layer and in upper layer, while with increase of Ra, number of pairs of counter-rotating convection rolls increases both in two layers and this directly leaves a major impact on isotherms . This can be explained by the following fact. With increase of Ra, viscosity of the fluids decreases. As a result, fluids particles can be separated from the bottom and top surfaces much easier which causes to have more numbers of convection rolls.

To make sure that the temperature gradient at hot wall changes with Ra, Nu_{avg} has been calculated for all cases. Its value for Rayleigh numbers of 2×10^4, 5×10^4, 10^5 and 2×10^5 are 1.408, 2.367, 3.013 and 3.471, respectively. Hence, as the Rayleigh number is increased, the temperature gradient near the top wall becomes sharper.

B. Effect of Prandtl number ratio
To study the effect of Prandtl number ratio on streamlines and isotherms, the Capillary number, Rayleigh number and ε_1 are held fixed at 4×10^{-4}, 5×10^4 and 0.1, respectively and the Prandtl number ratio is varied from 1 to 0.33 by changing the thermal diffusivity ratio. The results are shown in Fig. 4. As it can be observed easily in Fig. 4, with decrease of Pr_r, in the upper layer, temperature field gets uniform and fluid convection becomes weaker. This is because when the Prandtl number of the upper layer becomes less than the lower layer, conduction dominates in the upper area while convection dominates more in the lower area.
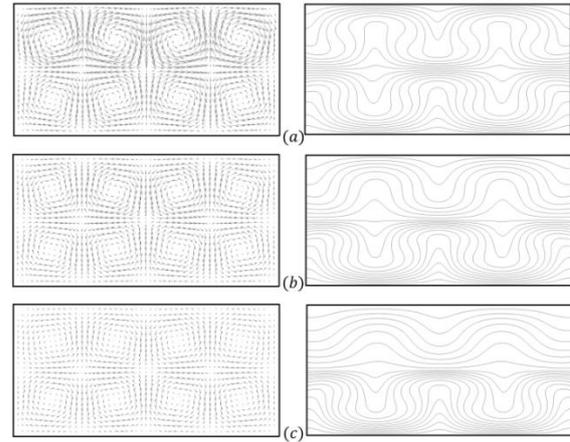

Fig. 4 Streamlines and isotherms for $Ra_h = 5.0 \times 10^4$, $Ca_h = 4.0 \times 10^{-4}$, $\varepsilon_h = 0.1$ (a) $Pr_r = 1.0$, (b) $Pr_r = 0.5$, and (c) $Pr_r = 0.33$

To investigate the effect of Pr_r on temperature gradient in bottom and top walls, average Nusselt numbers at both walls are shown in Table III. As can be seen, with decrease of Prandtl number ratio, Nu_{avg} at cold wall decreases while its value at hot wall increases.

Table III Average Nusselt Number at Hot And Cold Walls For Different Values Of Pr_r With $Ra_h = 5.0 \times 10^4$, $Ca_h = 4.0 \times 10^{-4}$, $E_h = 0.1$

Prandtl Number ratio	1.0	0.5	0.33
Nu_{avg} at hot wall	2.326	2.784	2.902
Nu_{avg} at cold wall	2.329	1.404	0.965

C. Effect of Parameter ε
To understand the effect of ε on isotherms and streamlines, for $Ra_h = 8 \times 10^4$, $Ca_h = 4 \times 10^{-4}$, $Pr_r = 1.0$ and different values of ε_h, isotherms and streamlines are plotted in Fig. 5.
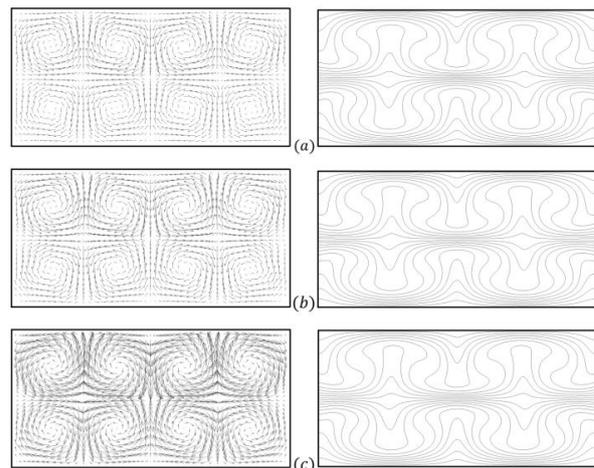

Fig. 5 Streamlines and isotherms for $Ra_h = 8.0 \times 10^4$, $Ca_h = 4.0 \times 10^{-4}$, $Pr_r = 1.0$ (a) $\varepsilon_h = 0.067$, (b) $\varepsilon_h = 0.1$, and (c) $\varepsilon_h = 0.2$

As it is obvious in Fig. 5, with increase of ε_h, circulation in the entire domain becomes stronger. This is because when the value of ε_h increases, the buoyancy force and then the fluid motion get stronger.

It should be noted that at a fixed value of Ra_h, with increase of ε_h, the viscosity of the fluid increases which impedes the fluid to circulate freely, but its effect isn't comparable with the effect buoyancy force. The effect of the parameter ε on the isotherms isn't distinguishable and in this case more data is needed. Therefore average Nusselt number at both cold and hot walls are calculated. The results are presented in Table IV.

Table IV Average Nusselt Number At Hot And Cold Walls For Different Values Of Eh With $Ra_h = 8.0 \times 10^4$, $Ca_h = 4.0 \times 10^{-4}$, $Pr_r = 1$

ε_1	0.067	0.1	0.2
Nu_{avg} at hot wall	2.784	2.802	2.802
Nu_{avg} at cold wall	2.795	2.800	2.801

No major change can be seen in average Nusselt numbers which indicates that parameter ε_1 does not have a major impact on the temperature field.

The flow velocity profiles on the horizontal mid-plane of the rectangular cavity for fixed values of Ra, Ca, ε, and Pr_r are given in Fig. 6.
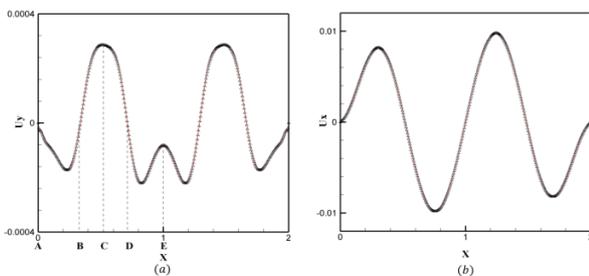

Fig. 6 Vertical (a) and Horizontal (b) velocity profiles on the horizontal midplane of the rectangular cavity for $Ra_h = 5.0 \times 10^4$, $Ca_h = 4.0 \times 10^{-4}$, $Pr_r = 1.0$, and $\varepsilon_h = 0.1$

IV. CONCLUSION

In the present study, simulation of two-phase Rayleigh-Benard problem in a rectangular cavity has been carried out using lattice Boltzmann method. To model the hydrodynamic and thermal fields, a new TLBM has been proposed which is indeed, the combination of isothermal LBM proposed by He et al. and a passive scalar approach. The numerical code was validated by the single-phase Rayleigh-Benard problem and a good agreement was observed. The effects of Rayleigh number, Prandtl number ratio and parameter ε were studied. It was found that with increase of Ra and ε, the fluid convection become stronger. Moreover, increase of Ra causes the isotherms to be more distorted while growth of ε does not leave a major impact on the isotherms. Also, with decrease of Pr_r, conduction gets dominated in the upper layer and as a result, the temperature field becomes uniform and the fluid motion gets weaker in this area. It was concluded that this new thermal lattice Boltzmann method is well capable of modelling the non-isothermal two-phase problems. Furthermore, since this method has the explicit feature and no solution of differential equation is involved, using this approach is much more convenient than traditional CFD methods.

REFERENCES

[1] T. Watanable, Flow pattern and heat transfer rate in Rayleigh–Benard convection, Physics of Fluids 16 (2004)

[2] M.C. Cross, P.C. Hohenberg, Pattern formation outside of equilibrium, Review of Modern Physics 65 (1993)

[3] C.W. Lan, M.C. Liang, M.K. Chen, Bifurcation and stability analyses for a two-phase Rayleigh-Benard problem in a cavity, Physics of Fluids 10 (6) (1998) 1329-1343

[4] B. Zhou, Q. Liu, Z. Tang, Rayleigh-Marangoni-Benard instability in two-layer fluid system, ActaMechanicaSinica/LixueXuebao 20 (4) (2004) 366-373

[5] Q.-S. Liu, B.-H. Zhou, Liu R., H. Nguyen-Thi, B. Billia, Oscillatory instabilities of two-layer Rayleigh-Marangoni-Benard convection, ActaAstronautica 59 (1-5) (2006) 40-45

[6] A. Prakash, J.N. Koster, Steady Rayleigh–Benard convection in a two-layer system immiscible liquids, Journal Heat Transfer 118 (1996)

[7] Ch. Jing, T. Sato, N. Imaishi, Rayleigh–Marangoni thermal instability in two-liquid layer system, Microgravity Science and Technology X (1) (1997)

[8] A. K. Gunstensen, D.H. Rothman, S. Zaleski, G. Zanetti, Lattice Boltzmann model of immiscible fluids, Physical Review A (1991) 43:4320–4327

[9] X. Shan, H. Chen, Lattice Boltzmann model for simulating flows with multiple phases and components, Physical Review E (1993)

[10] X. Shan, G. Doolen, Diffusion in a multicomponent lattice Boltzmann equation model, Physical Review E (1996) 54:3614–3620.

[11] M.R. Swift, W.R. Osborn, J.M. Yeomans, Lattice Boltzmann simulation of nonideal fluids, Physical Review Letters (1995)

[12] X. He, X. Shan, G.D. Doolen, Discrete Boltzmann equation model for nonideal gases, Physical Review E 1998

[13] X. He, G.D. Doolen, Thermodynamic foundations of kinetic theory and lattice Boltzmann models for multiphase flows, Journal of Statistical Physics (2002) 107:309–328

[14] X. He, S. Chen, R. Zhang, A lattice Boltzmann scheme for incompressible multiphase flow and its application in simulation of Rayleigh–Taylor instability, Journal of Computational Physics (1999) 152:642–663

[15] A. Fakhari, M.H. Rahimian, Simulation of falling droplet by the lattice Boltzmann method, Communications in Nonlinear Science and Numerical Simulation 14 (7) (2009) 3046-3055.

[16] F.J. Alexander, S. Chen, J.D. Sterling, Lattice Boltzmann thermo-hydrodynamics, Physical Review E 47 (1993) R2249.

[17] X. Shan, Simulation of Rayleigh—Bénard Convection Using a Lattice Boltzmann Method, Physical Review E 55 (1997) 2780–2788

[18] X. He, S. Chen, G.D. Doolen, 1998, A novel thermal model for the lattice Boltzmann method in incompressible limit, Journal of Computational Physics, 146

[19] O. Filipova, D. Hanel, 2000, A novel lattice BGK approach for low Mach number combustion, Journal of Computational Physics, 158

[20] Z. Guo, B. Shi, C. Zheng, 2002, A coupled lattice BGK model for the Boussinesq equations, International Journal of Numerical Methods in Fluids, **39**, 325.

[21] P. Yuan, L. Schaefer, A thermal lattice Boltzmann two-phase flow model and its application to heat transfer problems - Part 1. Theoretical foundation, Journal of Fluids Engineering, Transactions of the ASME128 (1) (2006) 142-150.

[22] P. Yuan, L. Schaefer, A thermal lattice Boltzmann two-phase flow model and its application to heat transfer problems - Part 2. Integration and validation, Journal of Fluids Engineering, Transactions of the ASME 128 (1) (2006) 151-156

[23] Q. Chang, J.I.D. Alexander, Application of the lattice Boltzmann method to two-phase Rayleigh-Benard convection with a deformable interface, Journal of Computational Physics 212 (2) (2006) 473-489

[24] N.F. Carnahan, K.E. Starling, Equation of state for no attracting rigid spheres, Journal of Chemical Physics (1959) 51(2):635

[25] T. Inamuro, M. Yoshino, H. Inoue, R. Mizuno, F. Ogino, A lattice Boltzmann method for a binary miscible fluid mixture and its application to a heat-transfer problem, Journal of Computational Physics 179 (1) (2002) 201-215

[26] R. M. Clever, F. H. Busse, Transition to time-dependent convection. Journal of Fluid Mechanics 65 (1974) 625-645.

[27] N. I. Prasianakis, I.V. Karlin, Lattice Boltzmann method for simulation of compressible flows on standard lattices, Physical Review E - Statistical, Nonlinear, and Soft Matter Physics, 78 (1) (2008) art. no. 016704